ELSEVIER

Chemical Engineering Journal 111 (2005) 53–61

Chemical Engineering Journal

www.elsevier.com/locate/cej

Ozone transfer and design concepts for NOM decolourization in tubular membrane contactor

T. Leiknes [a], J. Phattaranawik [a,b,*], M. Boller [b], U. Von Gunten [b], W. Pronk [b]

[a] *Department of Hydraulic and Environmental Engineering, NTNU Norwegian University of Science and Technology, S.P. Andersensvei 5, N-7491 Trondheim, Norway*

[b] *EAWAG Swiss Federal Institute for Environmental Science and Technology, Ueberlandstrasse 133, CH-8600 Duebendorf, Switzerland*

Received 29 November 2004; received in revised form 17 May 2005; accepted 20 May 2005

Abstract

Ozonation membrane contact was carried out with a tubular membrane module to study the effects of the flow rates and the temperatures of the liquid phase on ozone transfer and on the enhancement of mass fluxes. Changes in liquid temperature gave both positive and negative effects on the ozone fluxes for the nitrite solutions. The increase of the ozone fluxes with temperature was observed until the temperature approached approximately 40 °C. Ozonation membrane contact was also applied to decolorize Norwegian natural organic matter (NOM) at typical color concentrations in the range of 15–20 mg Pt/L. The ozone consumption for NOM decolourization tended to decrease with the liquid flow rates. A simple mass transfer model was proposed for the ozonation membrane contactor for the NOM decolourization studied here. The model was developed based on the concepts of the ozone consumption and the enhancement factor and can be used to describe the influence of mass transfer on the effluent colour concentration of the NOM. The experimental results validated the proposed model with deviations in the range of −9 to +7%. The decolourization rate constants obtained from the concentration–time (C–τ) model for the ozonation membrane contactor were found to be in the range of 139.44–298.81 $M^{-1}\,s^{-1}$. Simple concept to design ozonation membrane contactor for NOM decolourization was proposed. The kinetic characteristics for the NOM decolourization in ozonation membrane contactor are discussed in this paper.

Keywords: Membrane contactor; Ozone; Temperature effect; NOM decolourization; Design concepts

1. Introduction

Ozone is a strong oxidizing gas and offers a variety of reactions with both organic and inorganic substances due to the direct reaction with ozone and the indirect reaction with hydroxyl radicals formed during ozonation. Ozonation is applied in several environmental engineering processes for various purposes, for example disinfection of drinking water, oxidation of micropollutants, removal of odor, colour and particles. The benefit of ozone on environmental application is well-known and extensively discussed in the literature [1–3].

A conventional reactor to perform ozonation is a bubble column which is easy to set up and operate. However, some problems from bubble column have been found, for example flooding, uploading, emulsion, and foaming. These disadvantages can be defeated by using a gas–liquid membrane contactor [4].

Gas–liquid membrane contactor is a membrane process in which hydrophobic membranes (PTFE and PVDF) are used as a barrier to separate gas and liquid phases. The advantages of the membrane contactor over conventional contactors can be briefly shown as follows: (1) much higher interfacial area per volume is available than for conventional contactors, (2) higher mass transfer coefficients result in higher gas transfer rates and a smaller process volume for installation, (3) the effluent mixture gas (O_2/O_3) from membrane contactor can be more easily recycled back to the ozone generator

* Corresponding author at: Advanced Water and Membrane Center, Institute of Environmental Science and Engineering, Nanyang Technological University, Innovation Centre, Block 2 Unit 237, 18 Nanyang Drive, Singapore 637723, Singapore. Tel.: +65 6794 1514; fax: +65 6792 1291.

E-mail address: jirachote@ntu.edu.sg (J. Phattaranawik).

1385-8947/$ – see front matter © 2005 Elsevier B.V. All rights reserved.
doi:10.1016/j.cej.2005.05.007

Nomenclature

C	ozone concentration (mg/L)
d	inside diameter of tubular membrane (m)
D_{O_3-w}	diffusion coefficient of ozone in water (m^2/s)
E	enhancement factor (−)
H	Henry constant $((g/m^3)_G/(g/m^3)_L)$
J_{O_3}	ozone flux (g/m^2 s)
k_{dc}	NOM decolourization rate constant defined by Eq. (11) ($M^{-1}s^{-1}$)
k_G	mass transfer coefficient for gas stream (m/s)
k_L	mass transfer coefficient for liquid stream (m/s)
k_M	membrane transfer coefficient (m/s)
L	effective membrane lenght (m)
M	molar (mol/L)
N	number of fibers
Q_G	gas flow rate (L/h)
Q_L	liquid flow rate (L/h)

because of much lower moisture content, and (4) the ozone gas concentration at liquid–gas interface can be easily controlled at required values without the problems from flooding or uploading. More advantages of membrane contactor over a conventional bubble column have been reviewed in [4]. Additionally, contacting and mixing patterns of ozone gas and in the liquid stream in a membrane contactor are different from those in a conventional bubble column. Because contacting and mixing patterns can affect selectivity of series and parallel reactions [5], the membrane contactor can possibly give different reaction characteristics from the bubble column for some ozone-based reactions, such as ozonation of natural organic matter (NOM).

In order to achieve the optimum design criteria of the ozonation membrane contactor, the mass transfer in the tubular membrane contactor with and without a chemical reaction should be thoroughly studied. Therefore, this paper is intended to study the ozone transfer with and without a chemical reaction in the tubular membrane contactor. Nitrite solutions were used in this work, and the module was also used to decolorize Norwegian NOM, as a typical contaminant in Norwegian water source, to evaluate the performance of ozonation membrane contactor. The simple design equations and criteria were proposed in the paper. The kinetic details of the NOM decolourization by ozone were also evaluated and compared to the available literature.

2. Theory

Ozone transport in a gas–liquid membrane contactor from the gas phase through membrane into the liquid phase can be described by the resistance-in-series model, expressed by Eq. (1) [4]

$$\frac{1}{K_{L,O_3}} = \frac{1}{k_{G,O_3}H_{O_3}} + \frac{1}{k_{M,O_3}H_{O_3}} + \frac{1}{k_{L,O_3}} \quad (1)$$

The overall mass transfer coefficients with ozonation (K_{L,O_3}) can be measured from the experiments. k_{G,O_3} and k_{L,O_3} can be calculated from the available mass transfer correlations or measured from the oxygen transport experiments. The membrane mass transfer coefficient (k_{M,O_3}) can be evaluated by the dusty-gas model. The ozone solubility in pure water is evaluated by Henry's constants for the temperature range of 273–333 K with 10% mean error [6];

$$\log\left(\frac{H_{O_3}}{\text{kPa m}^3\,\text{mol}^{-1}}\right) = 5.12 - \frac{1230}{T(\text{K})} \quad (2)$$

When a chemical reaction occurs in the liquid phase, mass transfer resistance in the liquid boundary layer is reduced and mass transfer rate is enhanced. An increase of mass transfer rate due to a chemical reaction is quantified by the enhancement factor (E) defined by Eq. (3) [7].

$$E = \frac{J_{O_3}(\text{with reaction})}{J_{O_3}(\text{without reaction})} \quad (3)$$

The ozone fluxes (J_{O_3}) without a chemical reaction refer to the flux for pure water. The resistant-in-series model with a chemical reaction in the liquid phase in membrane contactor can be expressed by Eq. (4).

$$\frac{1}{K_{L,O_3}} = \frac{1}{k_{G,O_3}H_{O_3}} + \frac{1}{k_{M,O_3}H_{O_3}} + \frac{1}{k_{L,O_3}E} \quad (4)$$

In a gas–liquid membrane contactor, the resistance to mass transfer in the liquid boundary layer has been already proved to be the dominant step and can occupy more than 95% of overall mass transfer resistances [4,5] for the case of low-liquid Reynolds number and low gas solubility. As a result, the simpler model can be obtained when the mass transfer resistances in the membrane and in the gas phase are neglected, expressed in Eq. (5):

$$J_{O_3} = Ek_{L,O_3}\left(\frac{C_{G,O_3}}{H_{O_3}} - C_{L,O_3}\right) \quad (5)$$

Where C_{G,O_3} and C_{L,O_3} are the bulk concentrations of ozone in the gas phase and the liquid phase, respectively. $C_{G,O_3}/H_{O_3}$ is the ozone concentration in the liquid phase at the gas–liquid interface and also represents the driving force of ozone transfer in Eq. (5).

The effect of salt concentration on the ozone solubility can be evaluated by the Sechenov relation [6,8], and 500 mg/L nitrite solution lowered the ozone solubility by only 0.8%. The well-known Leveque mass transfer correlation (Eq. (6)) is commonly used to calculated the mass transfer coefficient in the liquid phase in membrane contactor.

$$\text{Sh}_L = \frac{k_L d}{D_{O_3-w}} = 1.62\left(\text{Re}\,\text{Sc}\frac{d}{L}\right)^{1/3} \quad \text{Re}\,\text{Sc}\frac{d}{L} \geq 10 \quad (6)$$

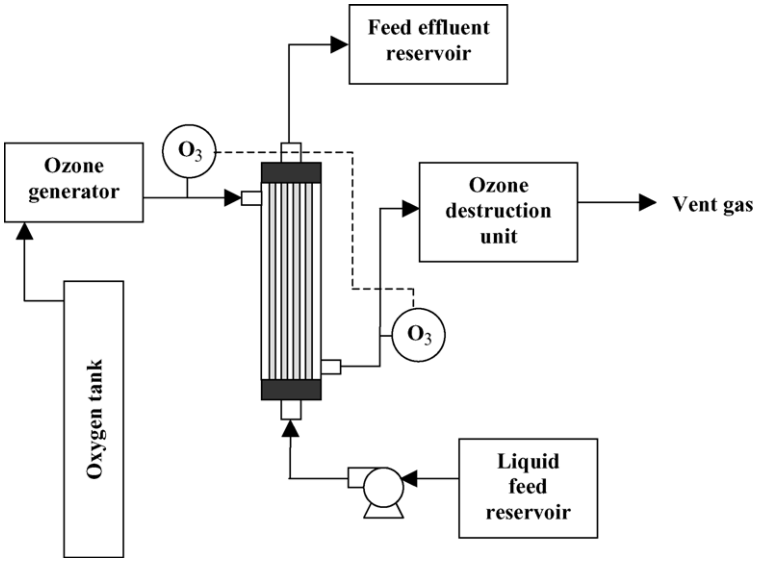

Fig. 1. Experimental apparatus diagram.

3. Experimental

There were two parts of the experiments. First, the ozone transfer experiments with pure water and 500 mg/L nitrite solutions were carried out to study the mass transfer characteristics of ozone in the tubular module, performed at NTNU (Norway). Second, the experiments for the NOM decolourization were performed at both NTNU and EAWAG (Switzerland) with the same module and the same experimental conditions to study the kinetic details of the NOM decolourization by ozone.

3.1. Ozone transfer experiments

The experimental setup diagram is exhibited in Fig. 1. The tubular PVDF membrane module (UMP-153) with Viton® seals was purchased from Pall Corporation. The properties of the membrane are listed in Table 1, and the module characteristics are summarized in Table 2. The housing material of the module is claimed to be polysulfone, which seems not to resist ozone. However, the resistance to ozone of the module was proved by using 100 mg/L ozone for 1 week before the main program of experiments was started.

Table 1
Membrane properties

Membrane material	Nominal pore size (μm)	Membrane porosity (ε)	Membrane thickness (μm)
PVDF	0.2	0.7	600

Pure oxygen (99.8%) was used in all experiments. The ozone gas was generated from the oxygen gas in a Laboratory Ozonizer 300 (Erwin Sander). The ozone concentrations in the gas stream were measured using an Ozone Analyzer BMT 961 (UV-photometric method) with a measurement uncertainty of 1.5%. The flow rate of the gas stream was 30 L/h, and the flow rates of the liquid stream ranged from 6 to 12 L/h, giving Reynolds numbers ranging from 16.4 to 32.8. The hydraulic retention times (τ) ranged from 9.9 to 39.7 s. The inlet ozone concentrations in the gas stream were set at 50 ± 0.2 mg/L for all experiments. The liquid temperatures were adjusted and controlled at the required values using a thermostatically controlled heater. (Lauda model E100). DI water was used to study the ozone transfer without a chemical reaction, while sodium nitrite ($NaNO_2$) solution at a concentration of 500 mg/L (7.2×10^{-3} mol/L) was utilized to study the ozone transfer accompanied with the oxidation in the liquid phase. The ozone fluxes for pure water were determined by mass balances on the liquid phase, while the ozone fluxes for the nitrite solutions were evaluated by the mass balances in the gas phase. The residual ozone concentrations in the aqueous solutions were determined by the indigo method [9,10].

3.2. NOM decolourization by ozonation membrane contactor

The experimental setup in this section at EAWAG was similar to that described above section except that an Anseros OEM ozone detector and an Ozonia ozone generator were used. The NOM solutions in this study was prepared by

Table 2
Module characteristics

Fiber i.d. (mm)	Fiber o.d. (mm)	Effective module length (mm)	Internal specific area (m^2/m^3)	Internal interface area (m^2)	Number of fibers
2.6	3.8	200.3	1534.8	0.084	50

mixing the NOM concentrate from the ion exchange unit in the drinking water plant (Meraker community, Norway) with DI water. The NOM concentrate was removed from the plant by using the concentrate NaOH solution, and pH of the NOM concentrate was 13.6. The pH of the NOM solutions was adjusted to pH 7 by 0.1 M H_2PO_4 solution. The decolourizations of the NOM solutions were monitored by measuring the colour unit (mg Pt/L) at UV wavelength 410 nm [11] (Norwegian standard method). The initial colour concentrations of the NOM solutions and dissolved organic carbon (DOC) were 18.6 ± 0.17 mg Pt/L at pH 7.0 ± 0.1 and 2.66 ± 0.4 mg/L, respectively. The initial UV absorbance at 254 nm was $14.8 \pm 0.9\ m^{-1}$.

4. Results and discussions

The average variation in the ozone flux measurements was approximately 5.1% in each repeated experiment. The residual ozone concentrations in the water were measured in triplicate, and the average variation was found at 6%. The average standard deviation in the spectrophotometric measurements for the NOM solutions and the indigo reagent I was about 2.8%. The average values of the experimental results are shown in Figs. 3–9.

4.1. Ozone transfer in membrane contactor

The tubular membrane module UMP-153 (Pall Company) served the experiments well. Although, the module housing and potting materials were claimed to be polysulfone and normal silicone epoxy, respectively, they resisted ozone gas through the experimental period 5 months.

The theoretical ozone decompositions in pure water in the membrane module at temperatures 20 and 40 °C at various flow rates are displayed in Fig. 2. At lower flow rates, the theoretical ozone decompositions are higher because longer hydraulic retention times. The maximum theoretical ozone

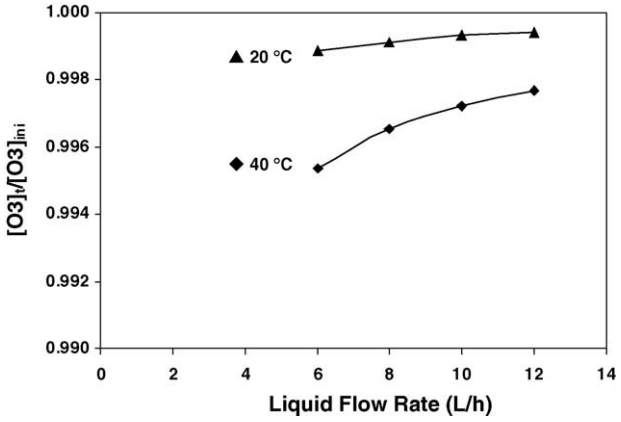

Fig. 2. Theoretical ozone decay in membrane contactor for liquid bulk temperatures 20 and 40 °C at various flow rates.

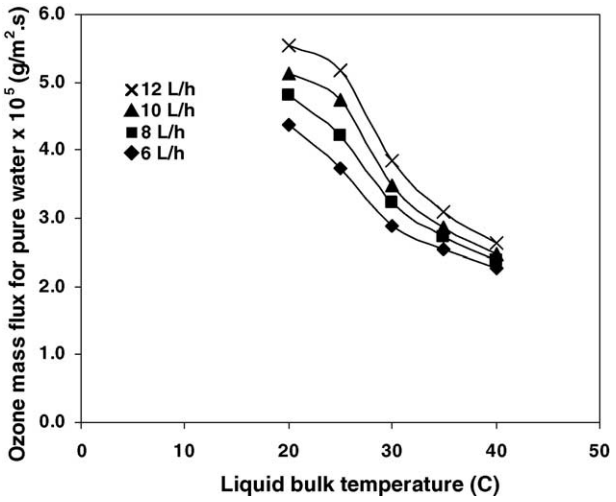

Fig. 3. Effect of temperatures and flow rates on ozone fluxes for pure water.

decomposition in pure water for this study was only 0.5%, which can be negligible.

Figs. 3 and 4 shows the ozone transfer in membrane contactor. The influences of liquid flow rates and bulk liquid temperatures on the mass fluxes of ozone gas for pure water are shown in Fig. 3. The mass fluxes of ozone decreased with increasing liquid bulk temperatures but increased with increasing flow rates. Lower ozone solubilities at higher temperatures resulted in lower concentration driving force in liquid phase (see Eq. (5)).

The opposite situations were found for the temperature effect when 500 mg/L $NaNO_2$ solutions were used in the system, shown in Fig. 4. The ozone fluxes increased with increasing bulk liquid temperatures until the temperatures approached 40 °C. When a fast chemical reaction takes place in the liquid phase, the temperature can have both negative and positive effects on the ozone fluxes. The reaction rate constant was enhanced by temperatures because lower acti-

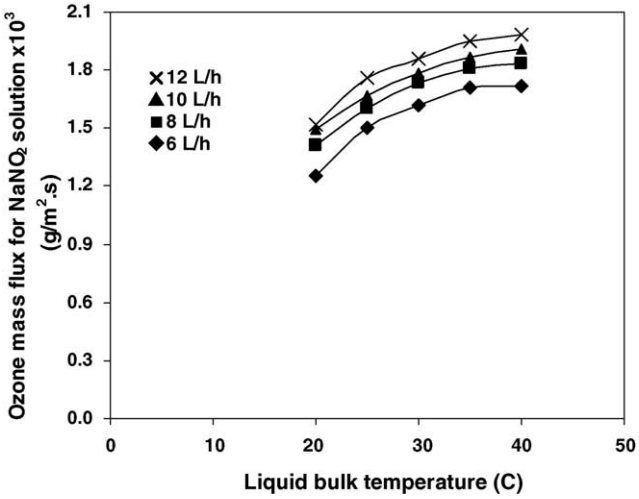

Fig. 4. Effect of temperatures and flow rates on ozone fluxes for 500 mg/L $NaNO_2$ solutions.

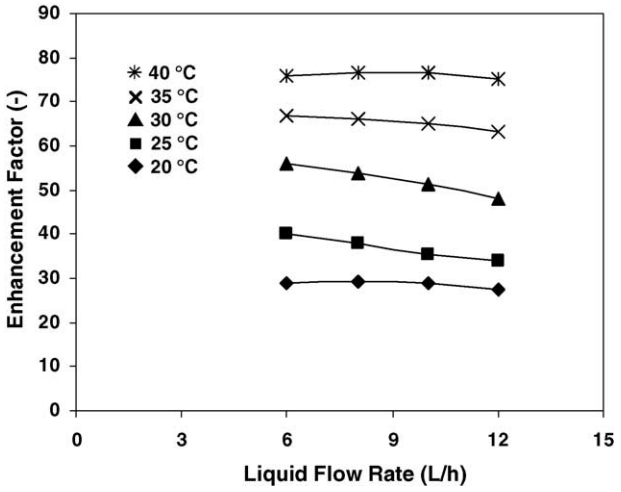

Fig. 5. Enhancement factors at various flow rates and temperatures for 500 mg/L $NaNO_2$ solution.

vation energy, while lower ozone solubility can reduce both ozone concentration involved in the reaction and concentration driving force in mass transfer. Thus, higher reaction rate constant was counter-balanced by lower ozone concentration in liquid and a lower mass transfer driving force at 40 °C. The positive effect of the temperature on the reaction rate constant dominated the ozone fluxes when the temperature was lower than 40 °C for the ozonation of nitrite to nitrate in this study. The enhancement factors (E) defined by Eq. (3) are shown in Fig. 5. The temperatures considerably increased the enhancement factors from 38 at 20 °C to 97 at 40 °C because the ozone fluxes into pure water decreased with increasing temperature, while the ozone fluxes into the nitrite solution increased with increasing temperature. The effect of liquid flow rates on the enhancement factors was relatively slight because increases of ozone fluxes with and without the reaction in similar magnitudes were obtained, and then E as the ratio of the fluxes with the reaction to the fluxes without the reaction slightly changed with the flow rates.

4.2. NOM decolourization and simple design concepts for ozonation membrane contactor

The observed ozone fluxes for the NOM solution were very close to the fluxes for pure water. The enhancement factors for the NOM solution ranged from 1.04 to 1.07% or from 4 to 7% flux enhancement. Thus, the observed enhancement factors were approximately 1. Low enhancement factors for ozonation of the NOM solutions were attributed by relatively low NOM concentrations together with low ozone concentrations in the solutions in molar unit. The dissolved ozone concentration at the gas–liquid interface was approximately 2.74×10^{-4} mol/L, and the NOM concentrations in molar unit can be roughly estimated from DOC, and NOM molecular weight, ranging from 2400 to 3900 [12] ([12] compared eight NOM taken from eight different lakes in Norway). Although NOM in [12] and NOM in this study were not taken from the same source in Norway, it would be reasonably assumed that NOM in this study has similar characteristics, and the molecular weight might be in the same range because those Norwegian NOM values are influenced by the same northern climate. Accordingly, the NOM concentrations in this study could be roughly 8.31×10^{-7} mol/L.

The residual ozone concentrations in the NOM solutions were lower than 0.05 mg/L. The results from the mass balance in the liquid phase show that the amounts of residual ozone leaving the module in the liquid phase were approximately 3–5% of total ozone transferred into the liquid phase. Hence, most ozone transferred into the liquid phase was consumed by the reactions in the NOM solutions before leaving the module, and the ozone concentrations in the bulk liquid approached zero when they are compared to the ozone concentration at the gas–liquid interface. In addition, more than one reaction should take place in the liquid phase, when the NOM solutions were employed. The possible reactions related to NOM can be written by Eqs. (7)–(9) for both direct and indirect reactions [13,14].

- Direct reaction:

$$O_3 + \text{NOM} \rightarrow \text{products from decolourization,}\quad k_{dc} \text{ for the decolourization rate constant} \tag{7}$$

$$O_3 + \text{NOM} \rightarrow \text{products from reaction with other function groups} \tag{8}$$

- Indirect reaction: chain reaction to accelerate ozone decomposition

$$O_3 + \text{NOM} \rightarrow OH^{\bullet} + \text{products} \tag{9}$$

Eq. (9) is an initiation step for ozone decomposition by NOM, please see [2,13] for more details. The locations of each reaction have not been identified yet. However, Hatta number (Ha) defined as the ratio of the rate of ozone consumed in the boundary layer to the rate of mass transfer across the boundary layer for reaction would be used to locate the regimes of the reactions.

$$\text{Ha} = \frac{\sqrt{k_{O_3} D_{O_3-w}}}{k_L} \in \tag{10}$$

Ha for ozonation of NOM can be estimated from the ozone decay with first-order reaction rate in NOM solutions, expressed in Eq. (10). The average value of the first-order rate constant for the ozone decay (k_{O_3}) in the NOM solution was $8.8 \times 10^{-3}\ s^{-1}$ taken from [15] in which overall reactions were included. Additionally, the rate constant was also in the similar range found in [14]. Mass transfer coefficients in the liquid phase (k_L) were calculated by Eq. (6).

The calculation results showed Ha for the ozone decay ranged from 0.52 to 0.82. Consequently, the reactions of ozone decay should be in the intermediate kinetic regime because $0.3 < \text{Ha} < 3$ [5,16,18] and occurred in both boundary

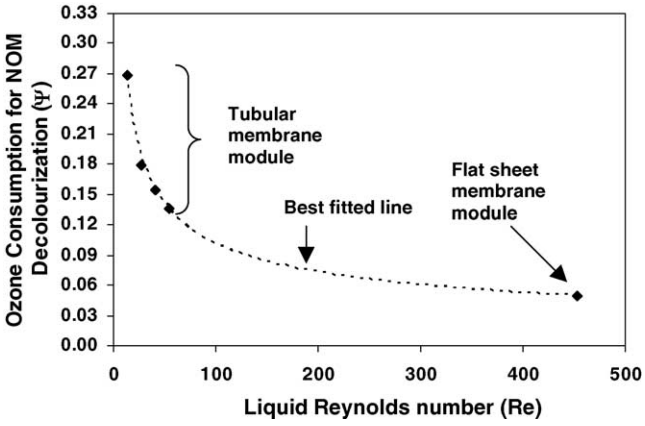

Fig. 6. Ozone consumptions at various Reynolds numbers.

layer and bulk. Thus, ozone can be consumed by the reactions Eqs. (7)–(9) in the bulk and in the boundary layer. However, bulk liquid would be likely to be main reaction zone because Ha is lower than 1 (mass transfer is faster than reaction rate in the film).

Mathematically, the magnitude of enhancement factor (E) mainly depends on reaction rates in the liquid film because reactions are likely to raise the effective ozone diffusivity [4] and mass transfer coefficient in the liquid film. If reactions in the film are fast, E should be much higher than 1 (see more detail in [5,18]). On another hand, if ozone decay in the NOM solution mainly takes place in the bulk liquid, E would be close to 1. Reactions in the bulk liquid can slightly increase ozone flux because of the slightly higher concentration difference which represents the driving force of ozone between interface and bulk (lower bulk concentration). As the results from Ha and E, main reaction zone of ozone reaction in NOM solution would be in the bulk liquid. However, it is very difficult to clearly identify the main regimes of each reaction, and more systematic investigation is required.

The ozone consumptions at various flow rates from the tubular membrane module at low Reynolds numbers (Re = 16–54) are shown in Fig. 6 together with the ozone consumptions from the flat sheet membrane module at higher Reynolds number (Re = 423) taken from [17]. The ozone consumptions were relatively higher than the average ozone consumption of NOM in conventional bubble columns at 0.1 mg O_3/mg Pt [1] when the Reynolds numbers were lower than 100. Interestingly, the ozone consumptions decreased with increasing Reynolds numbers from 0.27 mg O_3/mg Pt at Re = 13 to 0.05 mg O_3/mg Pt at Re = 453.

Ozone in the liquid phase could be consumed by the parallel reactions in Eqs. (7)–(9) or other possible parallel–series reactions. The reaction in Eq. (7) is responsible for the decolourization which can be detected by UV absorbance at 410 nm (Norwegian standard), while ozone can react with other functional groups in NOM molecules by direct reaction, expressed by Eq. (8). Indirect reaction (Eq. (9)) to accelerate the ozone decomposition in the NOM solutions provides $OH^{\bullet}$ radical which can be monitored by $OH^{\bullet}$ probe-ρCBA with HPLC. The ozone decay by the indirect reaction in NOM solution was proved to be significant [14,15]. Present work is supposed to focus only the decolourization, and the kinetic of NOM decolourization by ozone can be possibly analyzed by conventional concentration–time model ($C\tau$ model).

As in the case of the disinfection process, the exact properties of the NOM, such as molecular weight, structure, and reactivity with ozone are difficult to determine, so a simple model, such as Ct model in batch reactor is widely used. The C–τ model for NOM decolourization in ozonation membrane contactor as a continuous flow reactor (τ_L is liquid hydraulic retention time) is expressed in Eq. (11).

$$\ln\left(\frac{C^{\text{out}}_{\text{colour}}}{C^{\text{in}}_{\text{colour}}}\right) = -k_{\text{dc}}\,(C_L)\,\tau_L \tag{11}$$

where

$$\tau_L = \frac{N\pi d_i^2 L}{4Q_L}$$

In Eq. (11), the liquid hydraulic retention time (τ_L) is contact time for the decolourization. (C_L) is the ozone concentration (disinfectant) at where the reactions occurred. k_{dc} is NOM decolourization rate constant (which totally differs from k_{O_3} in Eq. (10)). However, the calculation results from Eq. (11), such as k_{dc} are not supposed to have general significance because k_{dc} can changes and varies with types and properties of NOM solution. Eq. (11) is supposed to provide only some concept for decolourization.

The ozone concentration in the boundary layer and the bulk for membrane contactor has to be redefined because it differs from conventional plug flow and batch reactors. For conventional plug flow reactor, such as bubble column, ozone in the liquid phase is continuously consumed along the liquid flow and considerably changed with the liquid retention time. As a result, the ozone concentration at the exit of bubble column is usually used in the $C\tau$ model for a continuous flow reactor. Differently, the reactor configuration of membrane contactor makes the ozone concentration at the gas–liquid interface relatively constant. In membrane contactor, fresh ozone is slowly introduced into the liquid phase along the module length, and the ozone concentration in the liquid phase at the gas–liquid interface depends on the ozone concentration in the gas phase. The calculation results in this study from Eqs. (14) and (15) show that the effluent ozone concentration in the gas phase is different from the inlet ozone concentration by only 7%, and the average ozone concentration in the gas phase is just 3.5% different from the inlet ozone concentration. If high ozone concentration, high flow rate of gas, and short module are employed, the ozone concentration in the gas phase is almost constant at the inlet concentration.

Fig. 7 displays the possible ozone concentration profiles in the reaction regimes in the bulk and boundary layer for the $C\tau$ model in a tubular membrane reactor. The reaction regimes cover both liquid boundary layer and the bulk. The average ozone concentration in the gas phase at the gas–liquid

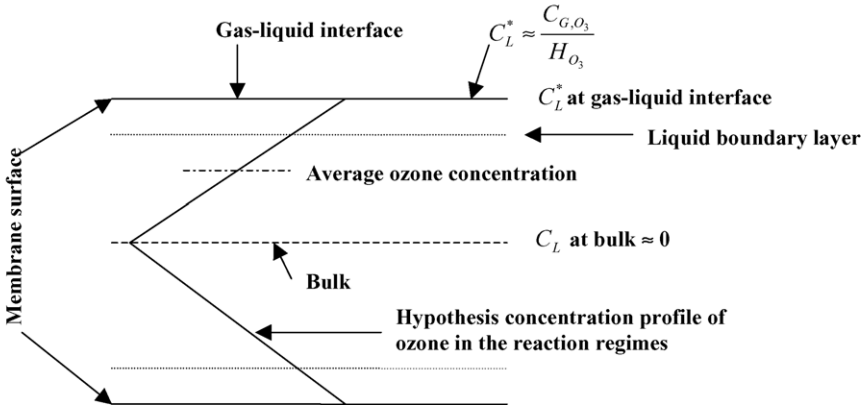

Fig. 7. Hypothesis diagram for ozone concentration in the reaction regimes in tubular membrane for Eq. (11).

interface along the membrane module can be calculated by Eqs. (14) and (15). Consequently, the ozone concentration in the liquid phase at the gas–liquid interface is approximately $\bar{C}_L^*/H_{O_3}$ when the resistances in the membrane and gas phase are negligible. The average ozone concentration in the reaction regimes in the bulk and the boundary layer is presumably $\bar{C}_L^*/2$ because the ozone concentration in bulk approached zero. Therefore, $(C_L) \approx \frac{\bar{C}_{G,O_3}}{2H_{O_3}}$.

Fig. 8 shows the decolourization rate constants of the NOM (k_{dc}) based on Ct concept in the tubular membrane contactor. The rate constants increased with liquid flow rates from 139.44 $M^{-1}\,s^{-1}$ at Re = 13.67 to 298.81 $M^{-1}\,s^{-1}$ at Re = 54.69. The obtained rate constants for Norwegian NOM decolourization were considerably lower than those of the typical inactivation rate constant for disinfection.

From above discussions, one conclusion can be drawn. The reaction characteristic of the NOM solutions is changed with respect to the Reynolds numbers or with respect to the mass transfer coefficient. Higher Reynolds numbers provided lower ozone consumptions and higher decolourization rate constants. Ozone could be consumed by the parallel reactions or parallel–series reactions, and selectivity for each reaction is probably varied with the Reynolds number. More ozone would be decayed by the chain reaction in Eq. (9) at lower flow rates. Higher decolourization rate constants were the evidence that the selectivity on the decolourization is higher at higher Reynolds numbers. Therefore, lower ozone decay should occur and made ozone more selective to the decolourization in Eq. (7) at higher flow rates. In practical application, high flow rate should be used because both low ozone decay and high flux can be obtained.

The possible reason for the lower ozone consumption is the difference in reactor configurations between bubble column and membrane contactor. Compared to a conventional bubble column, ozone transferred is slowly added into the liquid phase in membrane contactor. The difference in reactor configuration can lead to different reaction selectivity [5] and the appearance kinetic reaction would be changed. More detail and exact reason would be investigated in our next work.

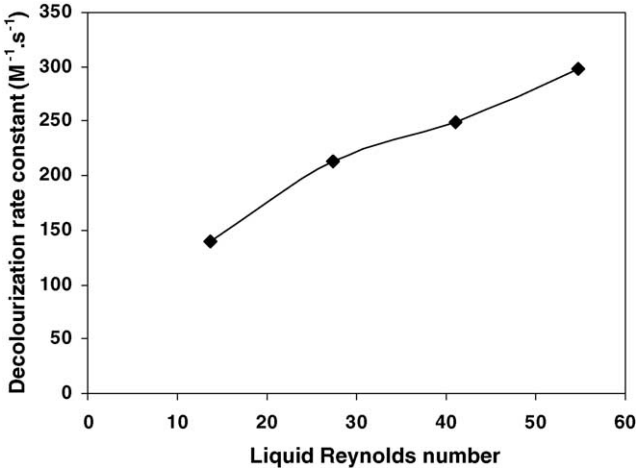

Fig. 8. Decolourization rate constants at various Reynolds numbers.

4.3. Design equations for NOM decolourization by ozonation membrane contactor

The design concepts for the NOM decolourization in ozonation membrane contactor can be developed based on the experimental results and simple mass balance in the membrane contactor. The simple mass balance in the membrane contactor for the NOM solution can be written by Eq. (12). The left hand side of Eq. (12) refers to amount of ozone transferred into the liquid phase, while the right hand side expresses the removal of the colour concentration of NOM by ozone. Ψ is the ozone consumption (mg of ozone consumed to reduce one colour unit or mg Pt/L), shown in Fig. 6.

$$Ek_L \frac{\bar{C}_{G,O_3}}{H_{O_3}} N\pi dL = Q_L \Psi (C_{colour}^{in} - C_{colour}^{out}) \quad (12)$$

Eq. (12) can be rewritten by Eq. (13).

$$C_{colour}^{out} = C_{colour}^{in} - \frac{Ek_L \bar{C}_{G,O_3}(N\pi\,dL)}{H_{O_3} Q_L \Psi} \quad (13)$$

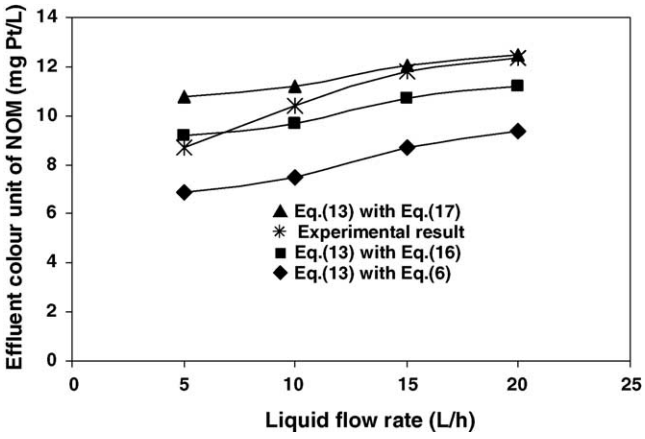

Fig. 9. Comparisons of calculation and experimental results for the effluent colour concentration of the NOM solutions.

where

$$\bar{C}_{G,O_3} = \frac{C^{in}_{G,O_3} + C^{out}_{G,O_3}}{2}$$

(average mass transfer driving force) (14)

and

$$C^{out}_{G,O_3} = C^{in}_{G,O_3} - \frac{Ek_L\bar{C}_{G,O_3}(N\pi\,dL)}{Q_G}$$

(from mass balance in gas phase) (15)

Eqs. (14) and (15) are used to calculate the average ozone concentration at the gas phase, which is then used to calculate the mass transfer driving force of ozone. The enhancement factor for the NOM solution can be assumed to be 1 as found from the experiments.

Prediction of effluent color concentration of NOM solution (C^{out}_{colour}) calculated by Eqs. (13) and (15) is shown in Fig. 9. Three mass transfer correlations (Eqs. (6), (16) and (17)) [20] were chosen to calculate mass transfer coefficients in Eq. (13). Those correlations are in Leveque's family of equations [20], which are commonly used to predict mass transfer coefficients in hollow fiber and tubular membrane modules. For calculation of mass transfer coefficients, diffusion coefficient of ozone in liquid is 1.26×10^{-9} m^2/s [17,19] and physical properties of pure water at the same temperature were presumably used as properties of the NOM solution since DOC of the NOM solution was low (only 2.6 mg/L). Theoretically, influence of the NOM on the viscosity of the NOM solution can be ignored [21] because mass fraction of the NOM in the solution was lower than 0.001%. In Fig. 9, the calculation results for predictions of the effluent colour concentration from Eq. (13) with Eqs. (16) and (13) with Eq. (17) show a good agreement with the experimental results, which are better than the prediction results from Eq. (13) with Eq. (6).

$$Sh_L = \frac{k_L d}{D_{O_3-w}} = 1.30\left(Re\,Sc\frac{d}{L}\right)^{1/3}, \quad Re\,Sc\frac{d}{L} \geq 10 \tag{16}$$

$$Sh_L = \frac{k_L d}{D_{O_3-w}} = 1.08\left(Re\,Sc\frac{d}{L}\right)^{1/3}, \quad Re\,Sc\frac{d}{L} \geq 10 \tag{17}$$

Please note that the data in Fig. 6 for ozone consumption and Eq. (12) are not complete, and more experiments are required to study the NOM characteristic for the ozone consumption. Fig. 6 and those design equations would be limited only for the initial colour concentrations of the NOM solutions between 18 and 22 mg Pt/L.

The $C\tau$ model in Eq. (11) can be combined with Eq. (13) to obtain new equation that can describe the influence of mass transfer coefficient and ozone consumption on the decolourization rate constants (k_{dc}). After substituting Eq. (11) into Eq. (13) and then rearranging, the decolourization rate constant for NOM decolourization based on $C\tau$ concept can be expressed as

$$k_{dc} = -\frac{1}{\left(\frac{\bar{C}_{G,O_3}}{2H_{O_3}}\right)\tau_L}\ln\left(1 - \frac{Ek_L\bar{C}_{G,O_3}(N\pi dL)}{C^{in}_{colour}H_{O_3}Q_L\Psi}\right) \tag{18}$$

5. Conclusions

Ozone transfer into pure water and the nitrite solution in the tubular membrane contactor was investigated. The influences of the liquid temperatures and flow rates on the ozone fluxes were studied. Increase in liquid temperature reduced ozone fluxes into pure water, but raised the ozone fluxes into $NaNO_2$ solutions. The increase of the ozone fluxes into $NaNO_2$ with the liquid temperatures was observed until the temperatures approached 40 °C because the counterbalancing effect between the rate constant and the concentration driving force was found. The tubular ozone membrane contactor was also used to decolourize the Norwegian NOM. High flow rates provided both low ozone decay and high ozone flux. The decolourization rate constants evaluated by the $C\tau$ model ranged from 139.44 to 298.81 M^{-1} s^{-1}. The simple mass transfer model was proposed to predict the effluent colour concentration and also used to design the membrane contactor. The proposed model gave a good agreement with the experimental results with average deviation of 4%.

Acknowledgement

The authors would like to thank American Water Work Association Research Foundation (AWWARF) for financial support.

References

[1] B. Langlais, D.A. Reckhow, D.R. Brink (Eds.), Ozone in water treatment: Application and Engineering, Lewis, Michigan, 1991.

[2] Urs Von Gunten, Review: Ozonation of drinking water. Part I. Oxiation kinetics and product formation, Water Research 37 (2003) 1443–1467.

[3] Urs Von Gunten, Review: ozonation of drinking water. Part II. Disinfection and by-product formation in presence of bromide, iodide or chlorine, Wat. Res. 37 (2003) 1469–1487.

[4] A. Gabelman, S.-T. Hwang, Hollow fiber membrane contactors, J. Membr. Sci. 159 (1999) 61–106.

[5] O. Levenspiel, Chemical Reaction Engineering, 3rd ed., Wiley, New York, 1999.

[6] E. Rischbieter, H. Stein, A. Schumpe, Ozone solubilities in water and aqueous salt solutions, J. Chem. Eng. Data 45 (2000) 338–340.

[7] W.P.M. Van Swaaij, G.F. Versteeg, Mass transfer accompanied with complex reversible chemical reactions in gas–liquid systems: an overview, Chem. Eng. Sci. 47 (1992) 3181–3195.

[8] S. Weisenberger, A. Schumpe, Estimation of gas solubilities in salt solutions at temperatures from 273 to 363 K, AIChE 42 (1996) 298–300.

[9] H. Bader, J. Hoigne, Determination of ozone in water by the indigo method, Wat. Res. 15 (1991) 449–456.

[10] American Public Health Association, American Water Works Association, and Water Environment Federation, Standard Methods for the Examination of Water and Wastewater, 20th ed., American Public Health Association, Washington, DC, 1998.

[11] Norwegian Standard Association, Norwegian standard: NS 4787: Water Quality: Determination of Colour Method by Spectrophotometric Determination Of Absorbance at 410 nm, 2nd ed., Norwegian Standard Association, Oslo, 2002.

[12] J.R. Lead, E. Balnois, M. Hosse, R. Menghetti, K.J. Wilkinson, Characterization of Norwegian natural organic matter: size, diffusion coefficients, electrophoresis mobilities, Environ. Int. 25 (1999) 245–258.

[13] J. Hoigne, H. Bader, Characterization of water quality criteria for ozonation processes. Part II. Lifetime of added ozone, Ozone Sci. Eng. 16 (1994) 121–134.

[14] H.-S. Park, T.-M. Hwang, J.-W. Kang, H. Choi, H.-J. Oh, Characterization of raw water for the ozone application measuring ozone consumption rate, Wat. Res. 35 (2001) 2607–2614.

[15] P. Westerhoff, G. Aiken, G. Amy, J. Debrox, Relationships between the structure of natural organic matter and its reactivity towards molecular ozone and hydroxyl radicals, Wat. Res. 33 (1999) 2265–2276.

[16] H. Benbelkacem, S. Mathe, H. Debellefontaine, Taking mass transfer limitation into account during ozonation of pollutants reacting fairly quickly, Wat. Sci. Technol. 49 (2004) 25–30.

[17] J. Phattaranawik, T. Leiknes, W. Pronk, Mass transfer studies in Flat-sheet membrane contactor with ozonation, J. Membr. Sci. 247 (2005) 153–167.

[18] F.J. Beltran, Ozone Reaction Kinetics for Water and Wastewater Systems, CRC Press, New York, 2004.

[19] C. Gottschalk, J.A. Libra, A. Saupe, Ozonation of Water and Waste Water: A practical guide to Understanding Ozone and its Application, Wiley–Vch, Morlenbach, 2002.

[20] L. Mi, S-T. Hwang, Correlation of concentration polarization and hydrodynamic parameters in hollow fiber modules, J. Membr. Sci. 159 (1999) 143–165.

[21] J.R. Welty, C.E. Wicks, R.E. Wilson, G. Rorrer, Fundamentals of Momentum, Heat and Mass Transfer, 4th ed., Wiley, New York, 2001.